Applied Catalysis B: Environmental 115–116 (2012) 16–24

Contents lists available at SciVerse ScienceDirect

Applied Catalysis B: Environmental

journal homepage: www.elsevier.com/locate/apcatb

Synthesis of cerium-doped MCM-41 for ozonation of *p*-chlorobenzoic acid in aqueous solution

Jishuai Bing, Laisheng Li*, Bingyan Lan, Gaozu Liao, Junyu Zeng, Qiuyun Zhang, Xukai Li

School of Chemistry & Environment, South China Normal University, Guangzhou 510006, China

ARTICLE INFO

Article history:
Received 28 September 2011
Received in revised form
26 November 2011
Accepted 14 December 2011
Available online 22 December 2011

Keywords:
Ce-MCM-41
Catalytic ozonation
p-Chlorobenzoic acid

ABSTRACT

Cerium-doped MCM-41 (Ce-MCM-41) was prepared by a hydrothermal method and its catalytic activity for ozonation of *p*-chlorobenzoic acid (*p*-CBA) in aqueous solution was studied. For comparison, cerium-loaded MCM-41 (Ce/MCM-41) was prepared by a dipping method. Ce-MCM-41 was characterized by the low and wide angle X-ray powder diffraction (XRD), nitrogen adsorption–desorption, transmission electron microscopy (TEM) and ultraviolet–visible diffuse reflection spectrum (UV–vis DRS). The results showed that the material retained the highly ordered mesopore structure of MCM-41 and had a surface area of 852 $m^2\,g^{-1}$. Cerium was incorporated into the framework of MCM-41, locating at tetrahedrally coordinated sites. The cerium doping content, initial pH of aqueous solution and reaction temperature played important roles in catalytic ozonation of *p*-CBA. Under the chosen conditions (1.39 $mg\,l^{-1}$ ozone dosage, 10 $mg\,l^{-1}$ *p*-CBA solution and 1 $g\,l^{-1}$ catalyst dosage), the high mineralization rate (86%) was achieved by Ce-MCM-41/O_3 process at 60 min reaction time, only 52% by O_3 alone. The combination of Ce-MCM-41 and O_3 exhibited a significant synergetic effect. Ce-MCM-41 showed the better activity and stability than cerium-loaded MCM-41(Ce/MCM-41) during catalytic ozonation of *p*-CBA, its cerium leaching was greatly reduced (only 0.085 $mg\,l^{-1}$) and below detection limit after being reused, compared with that of Ce/MCM-41 (0.44 $mg\,l^{-1}$) with the presence of the same theoretical cerium content. TOC removal rate slightly decreased from 86% to 81% and kept stable after Ce-MCM-41 being re-utilized two times, which illustrated that Ce-MCM-41 was a kind of promising catalyst for ozonation of *p*-CBA. The addition of Ce-MCM-41 significantly improved ozone decomposition into $HO^{\bullet}$ in aqueous solution and reduced ozone concentration in equilibrium.

1. Introduction

The marine and freshwater are polluted by anthropogenic halogenated organic compounds (such as solvents, pesticides and other industrial chemicals), which are often toxic, persistent and refractory [1]. Some persistent halogenated compounds were found in two typical marine aquaculture zones of South China [2]. As one kind of them, para-chlorobenzoic acid (*p*-CBA) was usually used as an intermediate for manufacturing dyes, fungicides, pharmaceuticals and other organic chemicals, especially as a probe compound for $HO^{\bullet}$ radicals due to its higher reactivity with hydroxyl radicals than ozone [3]. Removal of *p*-CBA in waters has drawn much attention from researchers in recent years [3–5]. Heterogeneous catalytic ozonation, a novel alternative to traditional AOPs, has received wide interests because of its potential effectiveness in the degradation and mineralization of refractory organic pollutants and lower negative effect on water quality [4,6]. Supported, unsupported metals and metal oxides are the most commonly used catalysts for the ozonation of organic compounds in waters, such as ZnO [3], MnO_2 [7], TiO_2 [8], Al_2O_3 [9], Ru/Al_2O_3 [10], Fe_3O_4-CoO/Al_2O_3 [11], Ni/AC [4], Fe/MCM-41 [12], Fe/SBA-15 and MnOx/SBA-15 [13,14]. As an important promoter, rare earth catalysts with special electronic structure have drawn much attention from researchers in recent years. Some literatures reported that Mn–Ce–O catalyst [15], Ce/AC [16] and nanostructured CeO_2 [17] presented the higher activity in catalytic ozonation process for TOC removal. In addition, CeO_2 could minimize bromate formation during ozonation of bromide-containing water [18].

The choice of catalyst support largely depends on its surface area and pore size. The higher surface area could provide more active sites, while the larger pore size easily allows the reactants to approach those catalytic active sites [19]. The commonly used catalyst supports include activated carbon, alumina etc. [10,16]. But the surface area of alumina is limited, and carbon materials are easily oxidized by ozone, which may lead to decreasing their activity [16,20]. A dipping method is often used to prepare catalyst, which is easy to stop up the passageway of the support and even leads to an unequal active constituent distribution [21]. The

* Corresponding author. Tel.: +86 20 39310185; fax: +86 20 39310187.
E-mail address: llsh@scnu.edu.cn (L. Li).

0926-3373/$ – see front matter © 2012 Elsevier B.V. All rights reserved.
doi:10.1016/j.apcatb.2011.12.017

regular, hexagonal mesoporous structure of MCM-41 and its potential modification by the introduction of specific metal cations or metal complexes have made MCM-41 an interesting material in chemical engineering, energy sources and environmental science [22,23]. However, most reports in environmental science include adsorption of VOCs [24–26] and heavy metals [27,28] by purely siliceous or metal modified MCM-41, while their catalytic activities for ozonation of organic pollutants in aqueous solution are scarcely reported [29]. In this work, cerium-doped MCM-41 was synthesized as a heterogeneous catalyst for ozonation process, and *p*-CBA was chosen as a model compound to analyze its catalytic activity.

2. Experimental

2.1. Chemicals and reagents

The sodium silicate ($NaSiO_3{\cdot}9H_2O$), cetyl trimethyl ammonium bromide (CTAB), sulfuric acid (H_2SO_4) and *p*-chlorobenzoic acid were purchased from Sinopharm Chemical Reagent Co. Ltd. (Shanghai, China). Cerium nitrate ($Ce(NO_3)_3{\cdot}6H_2O$), tert-butanol (TBA) and sodium hydroxide (NaOH) were from Tianjin Reagent Chemical Co. Ltd. (Tianjin, China). All chemicals were of analytical grade. Deionized water was used to prepare aqueous solution. Sulfuric acid and sodium hydroxide were added in aqueous solution to control its pH value.

2.2. Preparation of catalysts

Ce-MCM-41 was synthesized by a hydrothermal method. $Ce(NO_3)_3{\cdot}6H_2O$ was used as Ce source and $NaSiO_3{\cdot}9H_2O$ as silicon source [30]. Briefly, $NaSiO_3{\cdot}9H_2O$ (28.42 g) was dissolved in 70 ml deionized water stirring at 35 °C, a required quantity of $Ce(NO_3)_3{\cdot}6H_2O$, which was dissolved in 15 ml deionized water, was added to the above mixture and stirred for 15 min. The pH of the mixture was adjusted to 11 by using H_2SO_4 (2 mol l^{-1}) to form a gel. After stirring for 30 min, 7.28 g CTAB dissolved in 25 ml water, was added to the gel and stirred for another 30 min. Then the gel was transferred to a Teflon-lined steel autoclave and heated to 145 °C for 48 h. After natural cooling, the product obtained was filtered, washed several times with deionized water and dried at 80 °C for 12 h. The obtained sample was calcined at 550 °C for 6 h to remove the template. MCM-41 was prepared by the above procedure in the absence of $Ce(NO_3)_3{\cdot}6H_2O$.

Cerium-loaded MCM-41 (Ce/MCM-41) sample was prepared by an isovolumetric impregnation method. MCM-41 was first dried at 80 °C for 12 h. $Ce(NO_3)_3{\cdot}6H_2O$ was dissolved in deionized water to get a desirable concentration. MCM-41 (2 g) was dispersed into the above cerium solutions under ultrasonic vibration for 90 min. The mixture was dried at 80 °C, and then calcined at 550 °C for 6 h to obtain Ce/MCM-41. In order to study the morphology of cerium oxide and its contribution to catalytic ozonation of *p*-CBA, pure cerium oxide (CeO_2) was prepared at the same conditions as that of Ce-MCM-41, using $Ce(NO_3)_3{\cdot}6H_2O$ as a precursor.

2.3. Characterization of catalysts

Powder X-ray diffraction (XRD) measurements of the samples were carried out using Cu Kα radiation in the 2θ ranges of 1–10° (low angle) and 10–90° (wide angle) on a Rigaku D-MAX 2200 VPC X-ray diffractometer. The N_2 adsorption–desorption isotherms were carried out at 77 K on a Quantasorb surface area analyzer (Micromeritics, ASAP2020, USA). The surface area, pore size distribution, pore volume, and average pore diameter were determined by the BJH method. The pore size distribution was determined from the adsorption branch of the isotherm. The transmission electron microscopic (TEM) measurements were carried out using a JEOL electron microscope (JEM-2100), with an accelerating voltage of 120 kV. UV–vis DRS in the scale region (200–800 nm) were recorded on a Cary 5000 spectrophotometer using $BaSO_4$ pellet. The point of zero charge (pH_{pzc}) of MCM-41 and Ce-MCM-41 was estimated using potentiometric titration method [31].

2.4. Catalytic ozonation procedure

The catalytic reaction procedure was carried out in a 1.3 l cylindrical reactor (h = 500 mm, Φ_{in} = 60 mm) made of borosilicate glass. The reaction was maintained at the desirable temperatures by circulation water from a thermostatic bath (SDC-6, Ningbo, China). 1.3 l *p*-CBA around 10 mg l^{-1} (pH = 4.5) aqueous solution and 1.3 g catalyst were added into the reactor (slurry). Ozone was produced in situ from pure oxygen (1.2 l min^{-1}) by a DHX-SS-1G ozone generator (made in China), and ozone gas (100 mg h^{-1} output, its concentration in the gas was 1.39 mg l^{-1}) was fed into the solution through a porous glass plate at the bottom of the reactor. The excess ozone in the outlet gas was trapped by a $Na_2S_2O_3$ solution. Water samples were taken at regular intervals to analyze *p*-CBA and total organic carbon (TOC) concentration. The 5% $Na_2S_2O_3$ solution was used to quench the continuous ozonation reaction in the samples.

2.5. Analytical procedures

The pH of the aqueous solution was measured using a PHS-3B analyzer (made in China), with a combination pH electrode (E-201-C, made in China), which was calibrated with standard buffers. Ozone concentration in aqueous solution was measured by using the indigo method (25 °C, 1 atm) [32]. Water samples were firstly filtered by a 0.45 μm prefilter, and the concentration of O_3 was measured by V-5000 spectrophotometer (made in China) at 610 nm. The concentration of *p*-CBA was analyzed by means of a high performance liquid chromatography (HPLC, LC10A, Shimadzu, Japan) with a UV detector (SPD – 10AV) at 236 nm. A Diamonsil 5U C18 column (250 mm × 4.6 mm, Dikma technologies) was used. The mobile phase was a mixture of methanol and water at 70:30 (v/v), and its flow rate was 1.0 ml min^{-1}. TOC was measured by a Shimadzu TOC 5000 analyzer. The concentration of leaching cerium was detected by the inductively coupled plasma-atomic emission spectrometry (ICP-AES) (Thermo Scientific, IRIS Intrepid IIXSP, USA).

3. Results and discussion

3.1. Characterization of catalysts

The low angle XRD patterns of MCM-41 and Ce-MCM-41 were given in Fig. 1a. All samples exhibited a strong (1 0 0) diffraction peak at 2θ = 2.2°, other two low intensities (1 1 0) and (2 0 0) appeared at 2θ = 3.8° and 4.4°. These results indicated that MCM-41 structure was retained after the direct introduction of cerium into its framework [33]. Table 1 showed that the d_{100} values and unit cell parameters (a_0) slightly increased after the incorporation of cerium due to Ce^{4+} (the larger size) substituting Si^{4+}. When cerium ions were incorporated into the framework of MCM-41, its unit-cell parameter would increase. The introduction of cerium in MCM-41 also led to the decrease of its diffraction peak intensities, which indicated a relatively disordered mesopore structure arising from the doping of cerium. A similar situation was observed in MCM-41 containing other metal ions [33–35]. In addition, as seen from Fig. 1b, no diffraction peaks of cerium oxides crystal appeared in the wide angle XRD pattern of Ce-MCM-41. It illustrated that cerium was incorporated into the framework position

Table 1
Cell parameter, pore diameter, pore volume, pore wall and surface area of MCM-41 and Ce-MCM-41.

Sample	Si/Ce ratio	d_{100} (nm)	a_o (nm)[a]	S_{BET} ($m^2\ g^{-1}$)	Pore diameter (nm)[b]	Pore volume ($cm^3\ g^{-1}$)	Pore wall (nm)[c]
MCM-41	–	3.80	4.39	954.67	3.66	0.87	0.73
Ce-MCM-41	60	3.84	4.43	852.46	3.83	0.81	0.60

[a] $a_o = 2d_{100}/\sqrt{3}$.
[b] Pore diameter obtained from BJH analysis of desorption data.
[c] Pore wall = a_o – pore diameter.

and/or walls of MCM-41 mesoporous molecular sieve, which was similar to other observations [35].

The N_2 adsorption–desorption isotherms of MCM-41 and Ce-MCM-41 samples were shown in Fig. 2. All the samples provided the IV type isotherm of mesoporous materials with a sharp ramp in the relative pressure range of 0.25–0.35, which was due to the capillary condensation of nitrogen in the pores [33–35]. The pore diameter, pore volume, wall thickness, and surface area of MCM-41 and Ce-MCM-41 samples were presented in Table 1. The results showed that its surface area, pore volume and pore wall decreased when a certain amount of cerium was introduced in MCM-41 framework, but its pore size increased. These were attributed to the existence of cerium species in the channels. A similar result about incorporation of other metals (such as Co, La, Rh, etc.) into the silicate framework was reported [30,34,35]. Table 1 also showed MCM-41 sample had an average pore diameter of 3.66 nm, Ce-MCM-41 exhibited slightly wider pore size distribution than that of MCM-41. The results declared that Ce-MCM-41 retained a uniform mesostructure of MCM-41.

The TEM images of MCM-41 and Ce-MCM-41 samples were shown in Fig. 3. It could be clearly observed that both MCM-41 and Ce-MCM-41 samples exhibited well-ordered hexagonal arrays structure, which was conductive to organic compounds close to catalytic active site [36]. It could also be observed that there were not any particles containing cerium oxides on Ce-MCM-41 surface. It was believed that cerium was incorporated into the framework of MCM-41 [37].

Fig. 4 showed UV–vis DRS of MCM-41, Ce-MCM-41 and CeO_2. MCM-41 almost had no absorption in 250–450 nm region, CeO_2 had two absorption bands around 272 nm and 345 nm, and Ce-MCM-41 appeared an absorption band around 272 nm. Because the position of ligand to metal charge transfer (O^{2-}–Ce^{4+}) spectra depends on the ligand field symmetry surrounding Ce center, the electronic

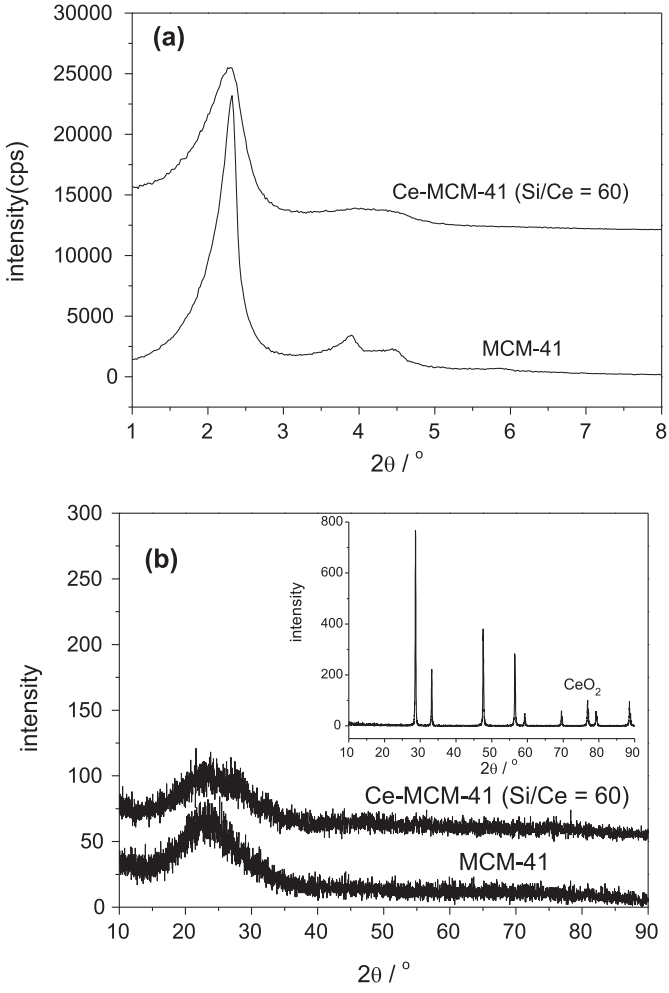

Fig. 1. (a) The low angle and (b) wide angle XRD pattern of different samples.

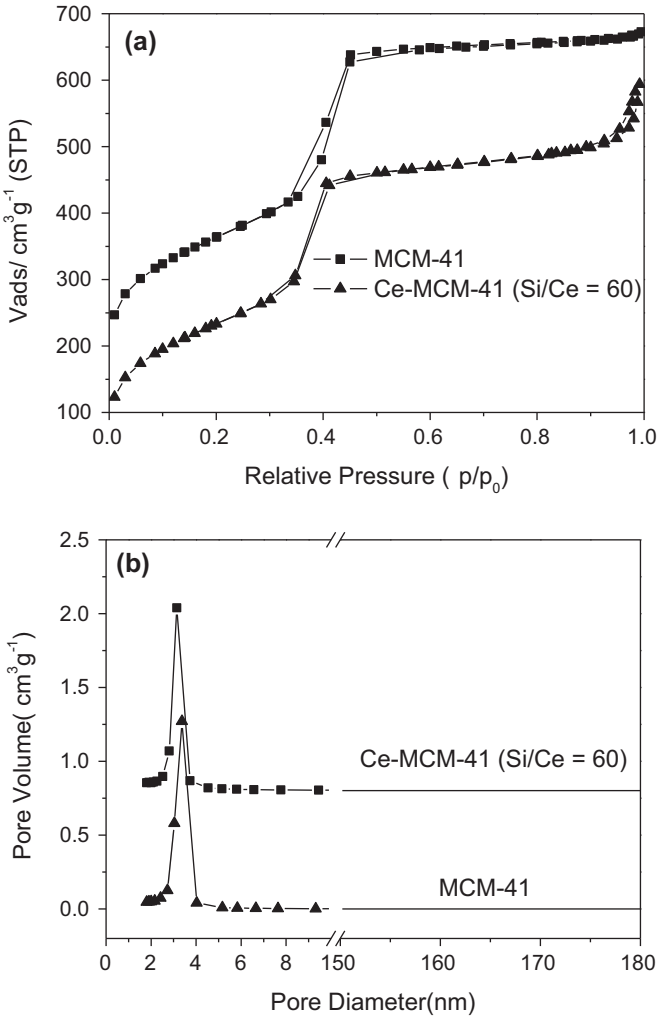

Fig. 2. (a) The N_2 adsorption–desorption isotherms and (b) pore size distribution curves of MCM-41 and Ce-MCM-41 (Si/Ce = 60).

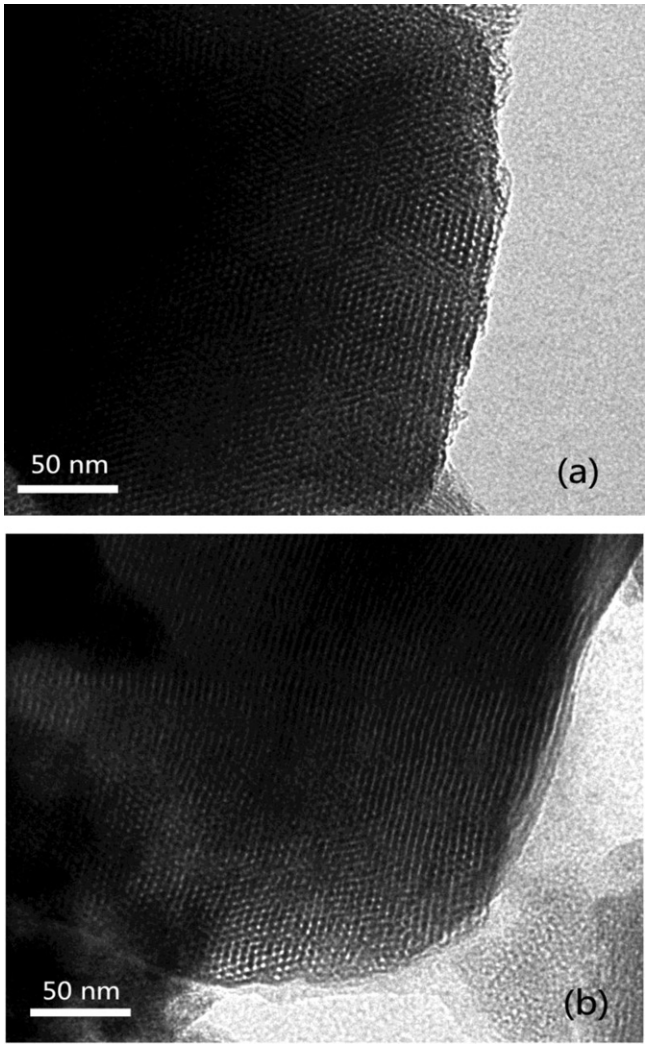

Fig. 3. TEM images of (a) MCM-41 and (b) Ce-MCM-41 (Si/Ce = 60).

transitions from oxygen to cerium require the higher energy for a tetra-coordinated Ce^{4+} than for a hexa-coordinated one. It could be inferred that the absorption peak around 272 nm was ascribed to the presence of the tetrahedral Ce^{4+} ions in the framework, and the adsorption peak around 345 nm was ascribed to the presence of the hexa-coordinated Ce^{4+} species in the extra-framework. So

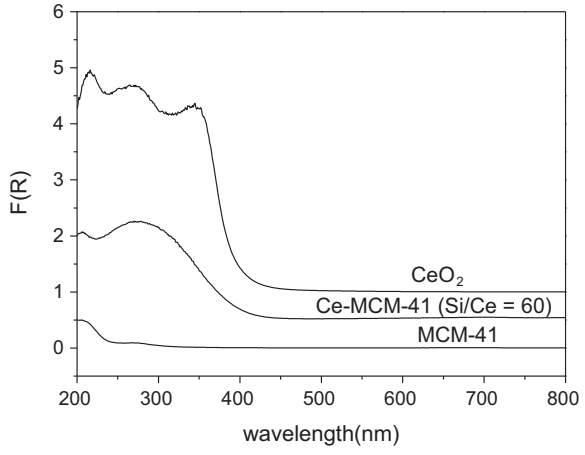

Fig. 4. UV–vis DRS of MCM-41 and Ce-MCM-41 (Si/Ce = 60).

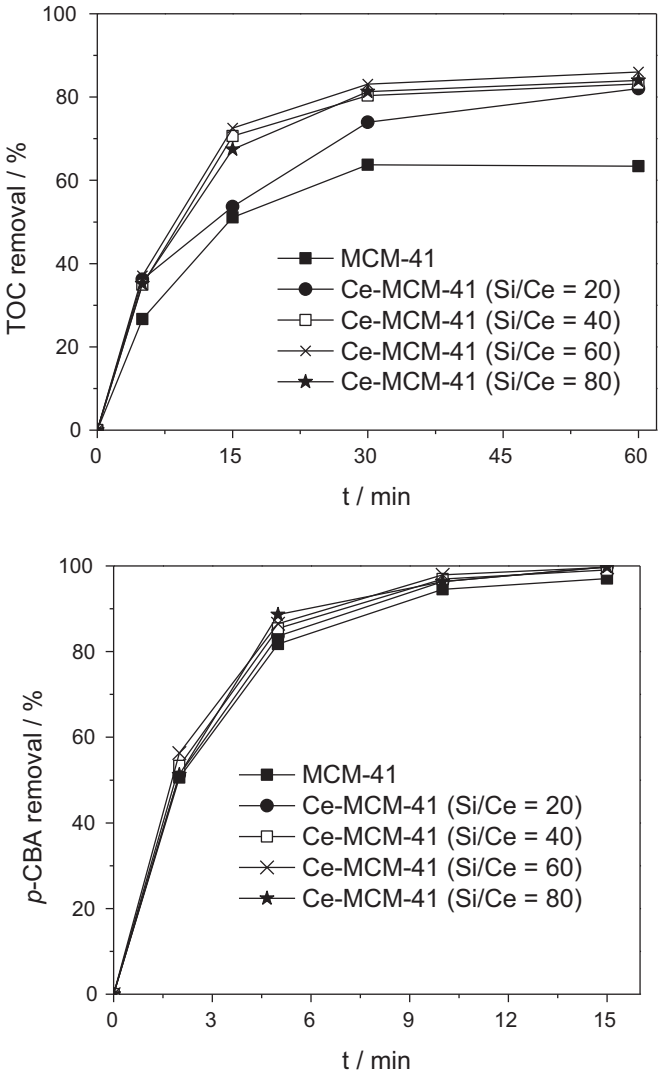

Fig. 5. Effect of cerium doping amount on *p*-CBA and TOC removal. Ozone dose: 100 mg h^{-1}; flow rate of oxygen: 1.2 l min^{-1}; catalyst dose: 1.3 g; initial concentration of *p*-CBA solution: 10 mg l^{-1}; volume of *p*-CBA solution: 1.3 l, temperature: 25 °C; pH = 4.5.

Ce^{4+} in Ce-MCM-41 framework mainly presented in tetrahedral coordination [33,35].

3.2. Effect of cerium doping content on Ce-MCM-41 catalytic activity

Fig. 5 provided *p*-CBA and TOC removal-time profile for ozonation of *p*-CBA by using Ce-MCM-41 as a catalyst. It could be observed that *p*-CBA was quickly removed in the oxidation system. The presence of Ce-MCM-41 slightly increased *p*-CBA conversion, but significantly improved *p*-CBA mineralization efficiency compared with the presence of MCM-41. The maximum TOC removal rate (86%) was obtained at 60 min when Si/Ce reached 60, only 63% with MCM-41.

Fig. 5 also exhibited the influence of cerium doping content (Si/Ce) on catalytic activity of Ce-MCM-41 for ozonation of *p*-CBA. TOC removal efficiency increased with Si/Ce ratio from 20 to 60, when Si/Ce ratio reached 60, TOC removal reached the maximum (86%). However, when Si/Ce ratio further increased up to 80, TOC removal was depressed. It was believed that the surface active sites of Ce-MCM-41 catalyst increased with cerium component [38]. However, overdoped cerium species would result in the destroy

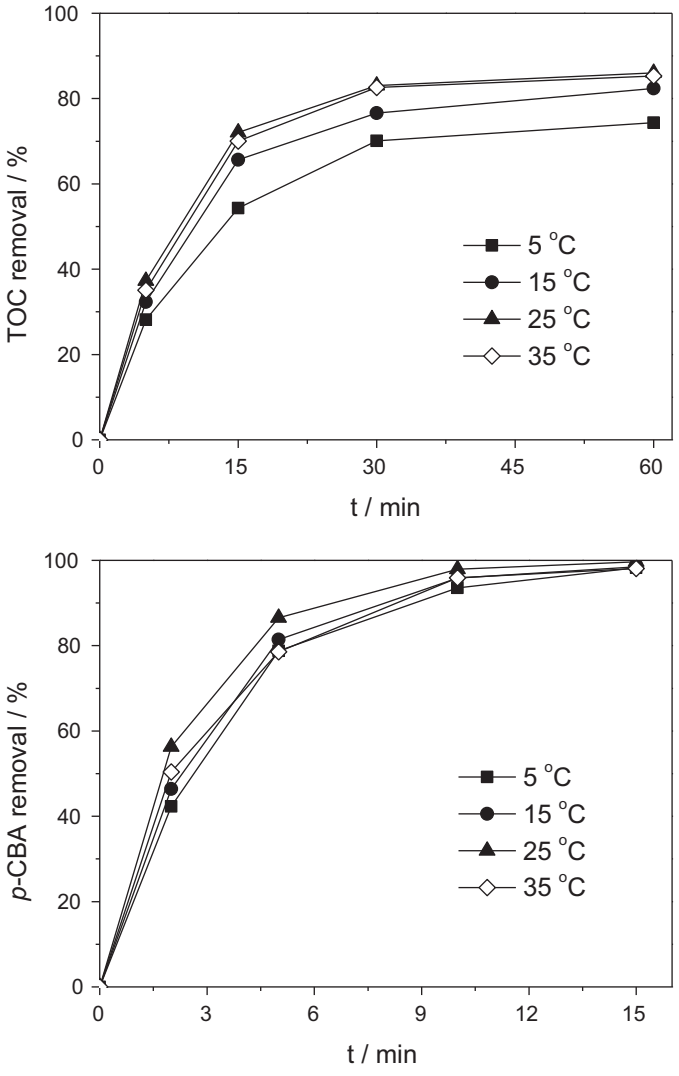

Fig. 6. Effect of reaction temperature on *p*-CBA and TOC removal. Ozone dose: 100 mg h^{-1}; flow rate of oxygen: 1.2 l min^{-1}; catalyst dose: 1.3 g; initial concentration of *p*-CBA solution: 10 mg l^{-1}; volume of *p*-CBA solution: 1.3 l; pH = 4.5.

of well ordered mesoporous structure and decrease the catalyst's surface area (confirmed by Table 1) and active sites, its catalytic activity would be depressed. As a result, cerium content played an important role in catalytic ozonation of *p*-CBA over Ce-MCM-41, and Si/Ce ratio of 60 was employed in the following experiment section.

3.3. Effect of reaction temperature on catalytic ozonation of *p*-CBA

Reaction temperature is an important factor since it influences gas solubility in waters, chemical reaction rate and chemical equilibrium [39,40]. Fig. 6 presented the effect of reaction temperature (5, 15, 25 and 35 °C) on catalytic activity of Ce-MCM-41 for ozonation of *p*-CBA. TOC and *p*-CBA removal increased with temperature from 5 °C to 25 °C, but further increased up to 35 °C, their removal was depressed.

Table 2 showed the effect of reaction temperature on the kinetics of *p*-CBA and TOC removal in Ce-MCM-41/O_3 process. A good linearity was attained when the first-order rate constant values were plotted against various *p*-CBA and TOC (in the first 30 min) concentrations, which suggested that *p*-CBA degradation and mineralization were of apparent first-order kinetics.

Table 2
The apparent first-order rate constants of *p*-CBA and TOC removal in Ce-MCM-41/O_3 process.

T (°C)	*p*-CBA		TOC	
	k (min^{-1})	R^2	k (min^{-1})	R^2
5	0.2756	0.9978	0.0399	0.9736
15	0.2801	0.9938	0.0471	0.9394
25	0.3697	0.9994	0.0589	0.9446
35	0.3655	0.9956	0.0584	0.9608

There are two opposite effects of increasing reaction temperature in catalytic ozonation process. On one hand, increasing reaction temperature can yield higher chemical reaction rate, which directly improves *p*-CBA degradation and mineralization efficiency. Besides, *p*-CBA was weakly ionized at pH 4.5 in aqueous solution, and the ionized *p*-CBA could increase ozone decomposition into hydroxyl radical [5]. The ionization of *p*-CBA was an endothermic reaction, and its ionized amount would increase with reaction temperature. So *p*-CBA mineralization efficiency was increased with reaction temperature from 5 °C to 25 °C. On the other hand, the increase of temperature would also lead to a decrease of the ozone solubility in aqueous phase [41], which resulted in the decrease of ozone concentration and hydroxyl radicals generated in aqueous solution. As well known, the concentration of hydroxyl radicals was crucial for TOC removal [16]. The competition of the two opposite effects makes 25 °C the optimal reaction temperature for catalytic ozonation of *p*-CBA over Ce-MCM-41. And 25 °C was employed in the following experiment.

3.4. Comparison of *p*-CBA and TOC removal among different processes

Fig. 7 showed the comparison of *p*-CBA and TOC removal among different processes. The adsorption removal of *p*-CBA by MCM-41, CeO_2, Ce/MCM-41 and Ce-MCM-41 were about 11%, 5%, 7% and 4% in equilibrium, respectively. The ozonation of *p*-CBA led to 52% TOC removal at 60 min. The simultaneous use of ozone and MCM-41 slightly increased *p*-CBA removal, TOC removal was increased to 63% mainly due to the adsorption of *p*-CBA by MCM-41. In the CeO_2/O_3 process, 71% TOC removal was attained, but the adsorption removal of *p*-CBA by CeO_2 was only 5%, so cerium was an effective active component in catalytic ozonation of *p*-CBA. In Ce-MCM-41/O_3 process, TOC removal efficiency was considerably improved from 52% by ozonation alone to 86%, but only 4% TOC removal by Ce-MCM-41 adsorption. It indicated that there was a significant synergetic effect (between Ce-MCM-41 adsorption and ozonation alone) in Ce-MCM-41/O_3 process. Ce/MCM-41/O_3 process also had a significant TOC removal (82%) compared with ozonation alone (52%), but the leaching amount of cerium with the presence of the same theoretical cerium content was 0.44 mg l^{-1}, and 5.2 times higher than that of Ce-MCM-41/O_3 process (0.085 mg l^{-1}). These results showed that Ce-MCM-41 prepared by a doped method could effectively reduce the leaching of active content which affected the activity and reusability of the catalyst [15]. So Ce-MCM-41 presented the better catalytic activity than Ce/MCM-41 for ozonation of *p*-CBA in aqueous solution.

3.5. Stability of Ce-MCM-41 in catalytic ozonation

In order to investigate the stability of Ce-MCM-41, Ce-MCM-41 from the previous experiment was recycled and the results were shown in Table 3. It presented that *p*-CBA removal nearly maintained at a constant, TOC removal slightly decreased from 86% to 81% and kept stable after being reused two times, which

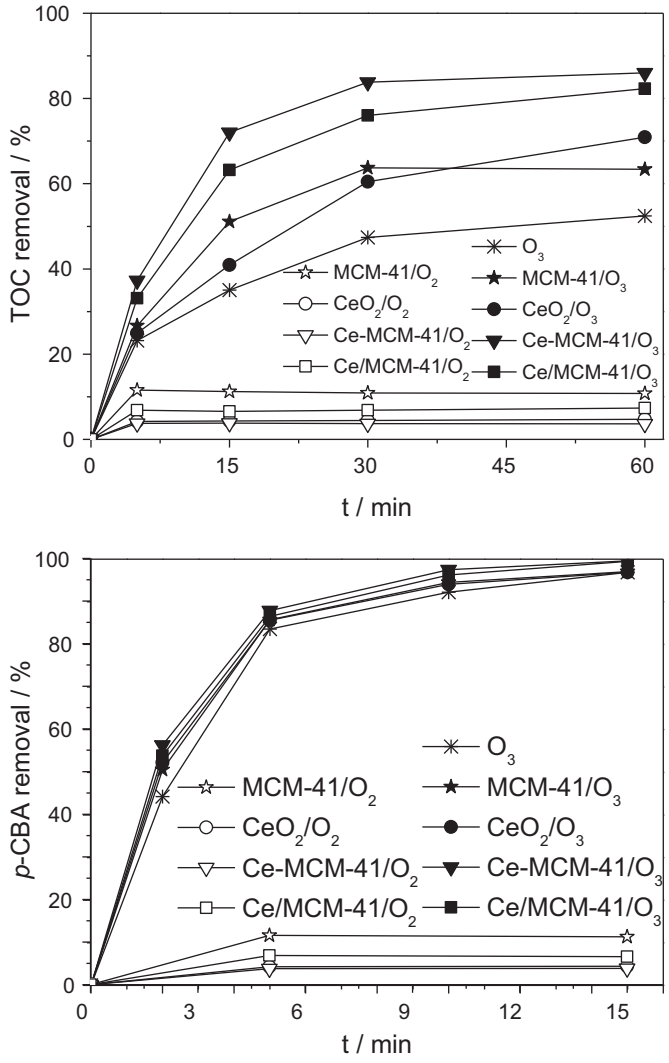

Fig. 7. Comparison of *p*-CBA and TOC removal by different processes. Ozone dose (if use): 100 mg h^{-1}; flow rate of oxygen: 1.2 l min^{-1}; catalyst dose (if use): 1.3 g; initial concentration of *p*-CBA solution: 10 mg l^{-1}; volume of *p*-CBA solution: 1.3 l; temperature: 25 °C; pH = 4.5.

Table 3
Stability of Ce-MCM-41 in catalytic ozonation process.

Number of repeated use	Ce-MCM-41 (Si/Ce = 60)	
	TOC (%)	*p*-CBA (%)
0	86	99.5
1	84	99.4
2	81	99.7
3	81	99.3

suggested that Ce-MCM-41 possessed an excellent activity and recyclability in the reaction. The effect of reused times of catalyst on cerium leaching in Ce-MCM-41/O_3 process (pH = 7.0, 60 min) was studied. A little leaching cerium (0.022 mg l^{-1}) was observed at the first use of Ce-MCM-41, and the leaching of cerium was below detection limit after being reused, which meant that the most of cerium was incorporated into the framework of MCM-41 and Ce-MCM-41 catalyst was provided with a good chemical stability and a long lifetime. It also illustrated that Ce-MCM-41 was a promising catalyst for ozonation of *p*-CBA in aqueous solution.

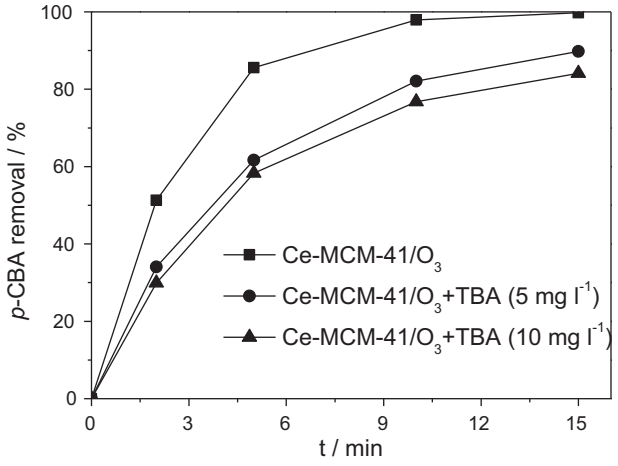

Fig. 8. Effect of TBA on catalytic ozonation of *p*-CBA. Ozone dose: 100 mg h^{-1}; flow rate of oxygen: 1.2 l min^{-1}; catalyst dose: 1.3 g; initial concentration of *p*-CBA solution: 10 mg l^{-1}; volume of *p*-CBA solution: 1.3 l; temperature: 25 °C; pH = 4.5.

3.6. Discussion on the mechanism

3.6.1. Effect of hydroxyl radical scavenger

Ozone reacts with various organic compounds in aqueous solution, either by the direct ozone selective reaction or indirect radical reaction involving HO• induced by ozone decomposition [41,42]. The reaction rate constant of *p*-CBA with HO• is 5.2×10^9 M^{-1} s^{-1}, but that with ozone is only 0.15 M^{-1} s^{-1} [3]. This illustrated that *p*-CBA was mainly degraded by HO• oxidation in ozonation alone and catalytic ozonation process.

TBA (tert-butanol) is a strong radical scavenger that has a reaction rate constant of 6.0×10^8 M^{-1} s^{-1} with hydroxyl radical and only 3.0×10^{-3} M^{-1} s^{-1} with ozone. At the same time, TBA cannot be adsorbed on the surface of metal oxides for its physical–chemical property [9]. In order to further prove whether the ozonation of *p*-CBA in the presence of Ce-MCM-41 involves HO• reaction, TBA was added into the reaction system. Fig. 8 showed that the presence of TBA markedly inhibited *p*-CBA degradation in Ce-MCM-41/O_3 process. At 15 min oxidation time, *p*-CBA removal efficiency reached 99.6% without TBA, only 89.7% with the presence of 5 mg l^{-1} TBA, 84.1% with 10 mg l^{-1} TBA. It suggests that the oxidation mechanism of *p*-CBA in Ce-MCM-41/O_3 process does occur via HO• in the liquid bulk.

3.6.2. Effect of adding catalyst on ozone concentration in aqueous solution

Fig. 9 showed ozone concentration variables with time in aqueous solution by O_3, MCM-41/O_3 and Ce-MCM-41/O_3 processes. It could be observed that ozone concentration in aqueous solution was very low at the first 5 min, owing to its quick reaction with *p*-CBA. After 30 min reaction time, ozone concentration in aqueous solution reached equilibrium. The ozone equilibrium concentration was 17.0 mg l^{-1} with ozonation alone, 9.3 mg l^{-1} with MCM-41/O_3 and 6.7 mg l^{-1} with Ce-MCM-41/O_3. These results illustrated that the addition of catalyst significantly increased ozone decomposition into HO• and reduced ozone equilibrium concentration in aqueous solution.

There are a lot of Si—OH groups on MCM-41 surface [43]. However, they did not have catalytic activity (confirmed by Fig. 7). The addition of MCM-41 just reduced ozone solubility in waters and could not accelerate ozone decomposition to generate hydroxyl radicals in the ozonation of *p*-CBA. The addition of Ce-MCM-41 presented the better catalytic activity than that of MCM-41 in the ozonation of *p*-CBA, because Ce-OH bonds were favorable sites to

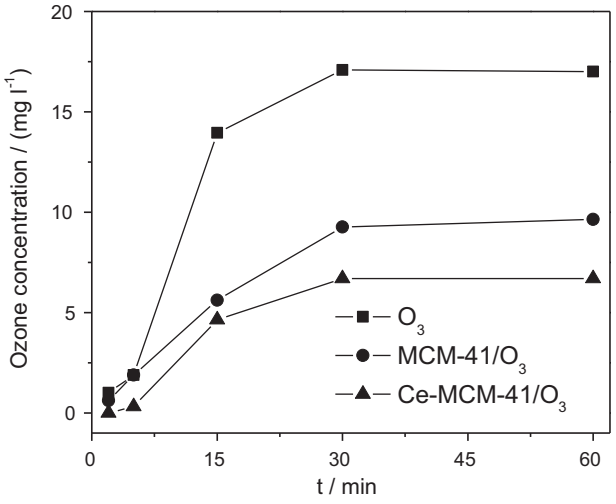

Fig. 9. Effect of adding catalyst on ozone concentration in aqueous solution. Ozone dose: 100 mg h^{-1}; flow rate of oxygen: 1.2 l min^{-1}; catalyst dose (if use): 1.3 g; initial concentration of *p*-CBA solution: 10 mg l^{-1}; volume of *p*-CBA solution: 1.3 l; temperature: 25 °C; pH = 4.5.

promote ozone decomposition into hydroxyl radical in aqueous solution [44].

3.6.3. Effect of initial pH on p-CBA degradation

In catalytic ozonation process, pH value of aqueous solution is an important factor which influences the generation rate of hydroxyl radicals, the utilization efficiency of ozone, the surface properties of catalyst, and charge of ionic or ionizable organic molecules [41,42]. The understanding of ozone decomposition at different pH is helpful for studying its reaction mechanism. According to the previous investigation, catalytic ozonation process occurs at three locations: (i) on the catalyst surface, (ii) at the catalyst/solution interface, and (iii) in the bulk solution. And the contribution of each part is various at different conditions [3,5,45]. In order to further delineate its reaction mechanism, ozonation and catalytic ozonation of *p*-CBA at different pH were investigated.

Fig. 10 illustrated the effect of initial pH (3.0, 5.0, 7.0, 9.0) on *p*-CBA and TOC removal in ozonation alone. It could be seen that *p*-CBA and TOC removal increased with initial pH from 3.0 to 9.0. At 60 min oxidation time, the maximum TOC removal (54%) was achieved at pH 9.0, only 53%, 51% and 47% at pH 7.0, 5.0 and 3.0, respectively.

The initial pH value of the aqueous solution was an important factor to affect the generation of hydroxyl radicals [41]:

$$O_3 + H_2O \rightarrow 2HO^\bullet + O_2, \quad k_2 = 1.1 \times 10^{-4}\,M^{-1}\,s^{-1} \qquad (1)$$

As shown in Eq. (1), the ozone molecule was one of the main reactive species in acidic and weakly acidic conditions, and *p*-CBA degradation exhibited a low efficiency. When pH was increased up to 7.0, the presence of OH^- could initiate ozone decomposition to form hydroxyl radicals, which had high reaction activity toward *p*-CBA ($k_{HO^\bullet}$, *p*-CBA = $5.2 \times 10^9\,M^{-1}\,s^{-1}$). But OH^- was a rather poor initiator of radical chain reaction ($k_{O_3,OH^-} = 70\,M^{-1}\,s^{-1}$) [41].

On the other hand, ozone decomposition was also affected by pH, which was related to the equilibrium concentrations of the dissociated forms of inorganic carbons (HCO_3^-/CO_3^{2-}) in an aqueous matrix. As shown in Eqs. (2) and (3), carbonate is a much stronger scavenger than bicarbonate [41,45]. Because the solution was prepared with distilled water, the concentration of inorganic carbon was low and the inhibiting impact of carbonate and bicarbonate on the oxidation process could be ignored.

$$HCO_3^- + HO^\bullet \rightarrow OH^- + {}^\bullet HCO_3, \quad k = 1.5 \times 10^7\,M^{-1}\,s^{-1} \qquad (2)$$

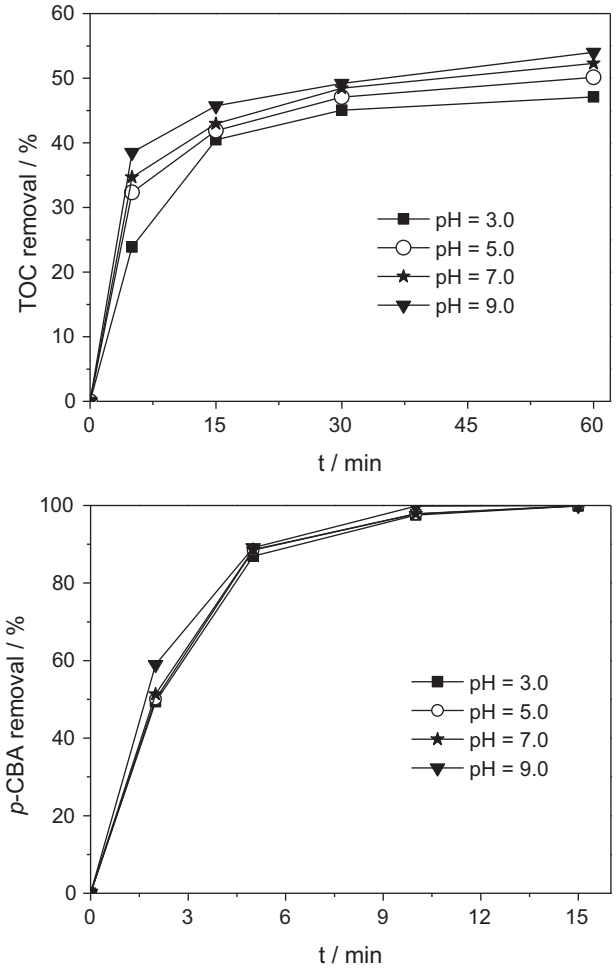

Fig. 10. Effect of initial pH of the solution on *p*-CBA and TOC removal in ozonation alone. Ozone dose: 100 mg h^{-1}; flow rate of oxygen: 1.2 l min^{-1}; initial concentration of *p*-CBA solution: 10 mg l^{-1}; volume of *p*-CBA solution: 1.3 l; temperature: 25 °C.

$$CO_3^{2-} + HO^\bullet \rightarrow OH^- + {}^\bullet CO_3^-, \quad k = 4.2 \times 10^8\,M^{-1}\,s^{-1} \qquad (3)$$

In addition, the amount of ionized *p*-CBA at various pHs was different through Eq. (4), and the ionized *p*-CBA could increase ozone decomposition into hydroxyl radical [5]. So *p*-CBA and TOC removal increased with pH in the ozonation process.

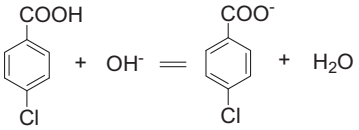

(4)

Fig. 11 provided the influence of initial pH (3.0, 5.0, 7.0, 9.0) of aqueous solution on *p*-CBA and TOC removal in Ce-MCM-41/O_3 process. The results showed that decreasing initial pH from 9.0 to 3.0 led to more TOC removal. At 60 min oxidation time, 89% TOC removal was achieved at pH 3.0, only 85%, 79% and 54% at pH 5.0, 7.0 and 9.0, respectively.

The hydroxyl groups on catalyst surface are believed to be crucial for the initiation of $HO^\bullet$ from ozone decomposition [44]. In acid condition, hydroxyl radicals were hardly generated from ozone decomposition in the bulk solution [41], but the surface properties of catalyst could help to generate hydroxyl radicals through Eqs. (5) and (6) [13,46].

$$M{-}OH_2^+ + O_3 \rightarrow M{-}OH^\bullet + HO^\bullet + O_2 \qquad (5)$$

$$M{-}OH^\bullet + H_2O \rightarrow M{-}OH_2^+ + HO^\bullet \qquad (6)$$

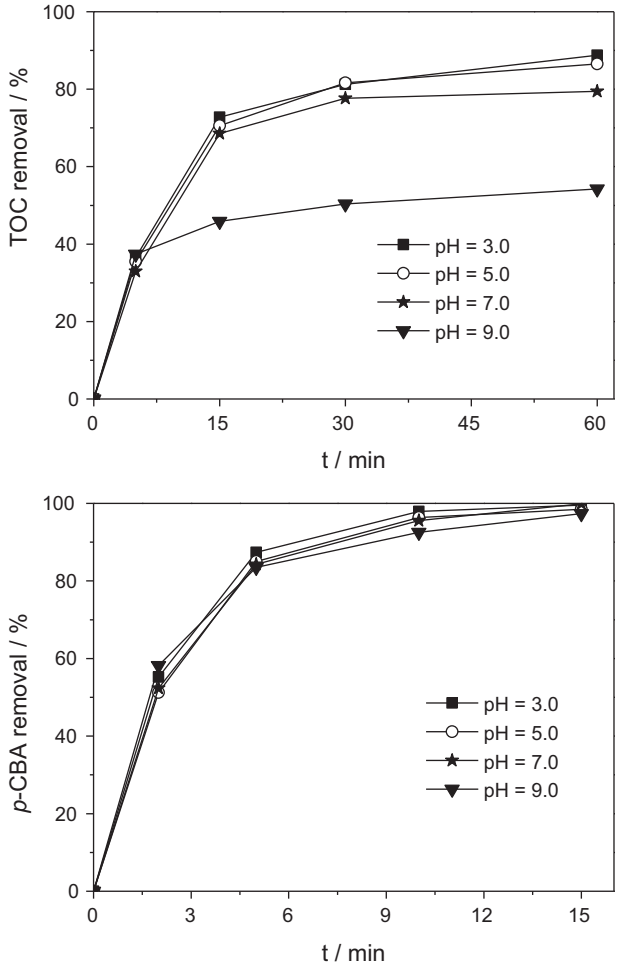

Fig. 11. Effect of initial pH of the solution on *p*-CBA and TOC removal in Ce-MCM-41 catalytic ozonation process. Ozone dose: 100 mg h^{-1}; flow rate of oxygen: 1.2 l min^{-1}; catalyst dose: 1.3 g; initial concentration of *p*-CBA solution: 10 mg l^{-1}; volume of *p*-CBA solution: 1.3 l; temperature: 25 °C.

In addition, the charge properties or acid/base properties of hydroxyl groups on catalyst surface could be changed with the conversion of pH_{pzc} and pH value of aqueous solution [42]. They could be inferred from Eqs. (7) and (8). Therefore, pH of the solution was an important factor that determined the charge properties of surface hydroxyl groups at catalyst/water interface [44].

$$MeOH + H^+ \Leftrightarrow MeOH_2^+ \quad (pH < pH_{pzc}) \tag{7}$$

$$MeOH + OH^- \Leftrightarrow MeO^- + H_2O \quad (pH > pH_{pzc}) \tag{8}$$

The pH_{pzc} of Ce-MCM-41 (Si/Ce = 60) was 6.10, which was much higher than that of MCM-41 (2.28). This meant that Ce-MCM-41 had higher basic group concentration than MCM-41. The basic groups on Ce-MCM-41 surface were primarily responsible for the enhanced ozone decomposition in aqueous solution due to its electrophilic characteristics [5]. When pH value was 3.0 and 5.0, the surface of catalyst had a positive charge as Eq. (7) shown, *p*-CBA was weakly ionized in aqueous solution with negative charge. Outer sphere complexes could be formed as a result of H-bond between carboxyl groups of *p*-CBA and hydroxyl groups of Ce-MCM-41 surface through Eq. (9). The sorbed *p*-CBA on Ce-MCM-41 surface reacted with HO• generated by ozone surface reaction through Eq. (10) [3]. However, as shown from Table 4, the leaching of cerium increased with solution acidity, which might decrease its catalytic stability. When cerium was doped into the silica framework of MCM-41, locating at tetrahedrally coordinated sites, a little cerium

Table 4
The effect of solution pH on leaching of cerium in Ce-MCM-41/O_3 process.

	Initial pH			
	3.0	4.5	7.0	9.0
$c_{(Ce)}$ (mg l^{-1})	0.86	0.085	0.022	0.022

leaching did not greatly change the surface property, which was crucial to generate HO• [44]. So pH played an important role in the sorption of *p*-CBA.

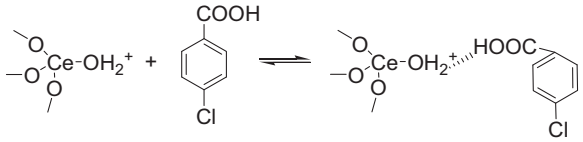

(9)

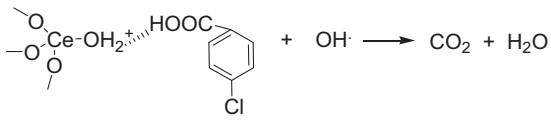

(10)

When pH was 7.0 and 9.0, the catalyst surface had a negative charge as Eq. (8) shown, *p*-CBA was not easily adsorbed on Ce-MCM-41 surface because of the electrostatic repulsion. The reaction at the catalyst/solution interface was inhibited. Combined with the results of both Figs. 10 and 11, TOC removal by O_3 alone and Ce-MCM-41/O_3 process at pH 9.0 confirmed the above statement, because their TOC removal was almost the same by O_3 alone and Ce-MCM-41/O_3 process. It implied that *p*-CBA degradation mainly occurred in the bulk solution at pH 9.0 and at the catalyst/solution interface in acidic conditions. So *p*-CBA with pH 3.0 and 5.0 in aqueous solution had much higher degradation effectiveness by Ce-MCM-41/O_3 process than that with pH 7.0 and 9.0.

4. Conclusion

Highly ordered MCM-41 and Ce-MCM-41 with uniform mesoporous structure were synthesized by a hydrothermal method. Cerium was incorporated into the framework of MCM-41, locating at tetrahedrally coordinated sites. The presence of Ce-MCM-41 slightly increased *p*-CBA conversion, but significantly improved the mineralization of *p*-CBA. The cerium doping content, reaction temperature and initial pH of *p*-CBA solution played important roles in Ce-MCM-41 catalytic ozonation of *p*-CBA. TOC removal efficiency reached 86% at 60 min oxidation time, 63% with MCM-41/O_3, 71% with CeO_2/O_3, 82% with Ce/MCM-41/O_3, and only 52% with ozonation alone. The leaching of cerium can be much more reduced using Ce-MCM-41 (0.085 mg l^{-1}) prepared by a doping method as a catalyst than Ce/MCM-41 (0.44 mg l^{-1}) prepared by an impregnation method. Ce-MCM-41 still maintained a good catalytic activity and stability after being reused three times (the leaching of cerium was below detection limit after being reused), TOC removal rate only slightly decreased 5% at 60 min reaction time, while *p*-CBA nearly kept to a constant rate. Ce-MCM-41 is a promising catalyst in the ozonation of *p*-CBA.

Acknowledgments

The authors are grateful for the financial support from the National Natural Science Foundation of China (Contract no. 20977036) and the Science & Technology Office of Guangdong Province (Contract no. 2010B030900006).

References

[1] M.M. Hägblom, V.K. Knight, L.J. Kerkhof, Environmental Pollution 107 (2000) 199–207.
[2] H.-Y. Yu, Y. Guo, L.-J. Bao, Y.-W. Qiu, E.Y. Zeng, Marine Pollution Bulletin 63 (2011) 572–577.
[3] H. Jung, H. Choi, Applied Catalysis B: Environmental 66 (2006) 288–294.
[4] X. Li, Q. Zhang, L. Tang, P. Lu, F. Sun, L. Li, Journal of Hazardous Materials 163 (2009) 115–120.
[5] J.-S. Park, H. Choi, J. Cho, Water Research 38 (2004) 2285–2292.
[6] A. Lv, C. Hu, Y. Nie, J. Qu, Applied Catalysis B: Environmental 100 (2010) 62–67.
[7] S.-p. Tong, W.-p. Liu, W.-h. Leng, Q.-q. Zhang, Chemosphere 50 (2003) 1359–1364.
[8] S. Song, Z. Liu, Z. He, A. Zhang, J. Chen, Y. Yang, X. Xu, Environmental Science & Technology 44 (2010) 3913–3918.
[9] F. Qi, Z. Chen, B. Xu, J. Shen, J. Ma, C. Joll, A. Heitz, Applied Catalysis B: Environmental 84 (2008) 684–690.
[10] Y. Zhou, W. Zhu, F. Liu, J. Wang, S. Yang, Chemosphere 66 (2007) 145–150.
[11] S. Tong, R. Shi, H. Zhang, C. Ma, Journal of Environmental Sciences 22 (2011) 1623–1628.
[12] R. Huang, J. Liu, L. Li, Q. Zhang, L. Zeng, P. Lu, Chinese Chemical Letters 22 (2011) 683–686.
[13] R. Huang, H. Yan, L. Li, D. Deng, Y. Shu, Q. Zhang, Applied Catalysis B: Environmental 106 (2011) 264–271.
[14] R. Rosal, M.S. Gonzalo, A. Rodríguez, J.A. Perdigón-Melón, E. García-Calvo, Chemical Engineering Journal 165 (2010) 806–812.
[15] R.C. Martins, R.M. Quinta-Ferreira, Applied Catalysis B: Environmental 90 (2009) 268–277.
[16] L. Li, W. Ye, Q. Zhang, F. Sun, P. Lu, X. Li, Journal of Hazardous Materials 170 (2009) 411–416.
[17] C.A. Orge, J.J.M. Órfão, M.F.R. Pereira, A.M. Duarte de Farias, R.C.R. Neto, M.A. Fraga, Applied Catalysis B: Environmental 103 (2011) 190–199.
[18] T. Zhang, W. Chen, J. Ma, Z. Qiang, Water Research 42 (2008) 3651–3658.
[19] S. Chaliha, K.G. Bhattacharyya, Industrial & Engineering Chemistry Research 47 (2008) 1370–1379.
[20] T.L. Rakitskaya, A.Y. Bandurko, A.A. Ennan, V.Y. Paina, A.S. Rakitskiy, Microporous and Mesoporous Materials 43 (2001) 153–160.
[21] X.-Y. Hao, Y.-Q. Zhang, J.-W. Wang, W. Zhou, C. Zhang, S. Liu, Microporous and Mesoporous Materials 88 (2006) 38–47.
[22] C.T. Kresge, M.E. Leonowicz, W.J. Roth, J.C. Vartuli, J.S. Beck, Nature 359 (1992) 710–712.
[23] N. Srinivas, V. Radha Rani, S.J. Kulkarni, K.V. Raghavan, Journal of Molecular Catalysis A: Chemical 179 (2002) 221–231.
[24] Q. Qin, J. Ma, K. Liu, Journal of Colloid and Interface Science 315 (2007) 80–86.
[25] H. Sepehrian, J. Fasihi, M. Khayatzadeh Mahani, Industrial & Engineering Chemistry Research 48 (2009) 6772–6775.
[26] D.P. Serrano, G. Calleja, J.A. Botas, F.J. Gutierrez, Industrial & Engineering Chemistry Research 43 (2004) 7010–7018.
[27] A. Benhamou, M. Baudu, Z. Derriche, J.P. Basly, Journal of Hazardous Materials 171 (2009) 1001–1008.
[28] K.M. Parida, S.K. Dash, Journal of Hazardous Materials 179 (2010) 642–649.
[29] M. Sui, J. Liu, L. Sheng, Applied Catalysis B: Environmental 106 (2011) 195–203.
[30] T. Somanathan, A. Pandurangan, D. Sathiyamoorthy, Journal of Molecular Catalysis A: Chemical 256 (2006) 193–199.
[31] J.P. Chen, S. Wu, K.-H. Chong, Carbon 41 (2003) 1979–1986.
[32] H. Bader, J. Hoign, Water Research 15 (1981) 449–456.
[33] Q. Zhao, Y. Xu, Y. Li, T. Jiang, C. Li, H. Yin, Applied Surface Science 255 (2009) 9425–9429.
[34] M. Boutros, F. Launay, A. Nowicki, T. Onfroy, V. Herledan-Semmer, A. Roucoux, A. Gédéon, Journal of Molecular Catalysis A: Chemical 259 (2006) 91–98.
[35] W. Zhan, G. Lu, Y. Guo, Y. Guo, Y. Wang, Journal of Rare Earths 26 (2008) 59–65.
[36] S. Chaliha, K.G. Bhattacharyya, Catalysis Today 141 (2009) 225–233.
[37] Q. Dai, X. Wang, G. Chen, Y. Zheng, G. Lu, Microporous and Mesoporous Materials 100 (2007) 268–275.
[38] L. Zhao, Z. Sun, J. Ma, H. Liu, Environmental Science & Technology 43 (2009) 2047–2053.
[39] H. Dehouli, O. Chedeville, B. Cagnon, V. Caqueret, C. Porte, Desalination 254 (2010) 12–16.
[40] L. Zhao, J. Ma, Z. Sun, H. Liu, Journal of Hazardous Materials 167 (2009) 1119–1125.
[41] B. Kasprzyk-Hordern, M. Ziólek, J. Nawrocki, Applied Catalysis B: Environmental 46 (2003) 639–669.
[42] L. Zhao, J. Ma, Z. Sun, X. Zhai, Environmental Science & Technology 42 (2008) 4002–4007.
[43] J. Trébosc, J.W. Wiench, S. Huh, V.S.Y. Lin, M. Pruski, Journal of the American Chemical Society 127 (2005) 3057–3068.
[44] T. Zhang, C. Li, J. Ma, H. Tian, Z. Qiang, Applied Catalysis B: Environmental 82 (2008) 131–137.
[45] J. Ma, M. Sui, T. Zhang, C. Guan, Water Research 39 (2005) 779–786.
[46] L. Zhao, Z. Sun, J. Ma, Environmental Science & Technology 43 (2009) 4157–4163.